Open access • Journal Article • DOI:10.1051/JP4:1996610

The Influence of the Back Stress (X) and the Hardening Rate (dX/Xεpqe) on Void Nucleation in α/β Titanium Alloys — Source link

A.L. Helbert, X. Feaugas, M. Clavel

Institutions: University of Technology of Compiègne

Published on: 01 Oct 1996 - Journal De Physique Iv (EDP Sciences)

Topics: Nucleation, Hydrostatic stress and Hardening (metallurgy)

The Influence of the Back Stress (X) and the Hardening Rate (dX/Xϵpqe) on Void Nucleation in α/β Titanium Alloys

A. Helbert, X. Feaugas, M. Clavel

JOURNAL DE PHYSIQUE IV
Colloque C6, supplément au Journal de Physique III, Volume 6, octobre 1996

The Influence of the Back Stress (X) and the Hardening Rate ($dX/x\varepsilon_{peq}$) on Void Nucleation in α/β Titanium Alloys

A.L. Helbert, X. Feaugas and M. Clavel

Université de Technologie de Compiègne, Division Mécanique, Laboratoire LG2mS, URA 1505 du CNRS, BP. 649, 60206 Compiègne cedex, France

Abstract: The study of void nucleation in four α/β titanium alloys has provided nucleation criteria corresponding to voids at the α/β interface. This macroscopic nucleation criterion, written as $\Sigma_m=f(\varepsilon_{peq})$, was explained with the help of microscopic observations. Microscopic parameters such as plastic strain in the α-phase or local hydrostatic stress σ_m at the α/β interface have been linked to the damage initiation. Besides, the influence of the different heterogeneity levels on the macroscopic nucleation criterion was demonstrated using the macroscopic mechanical parameters: back stress (X) and hardening rate ($dX/d\varepsilon_{peq}$) which express the plastic strain incompatibilities and their evolution in such alloys.

1. INTRODUCTION

Even if a lot of damage studies have been developed in alloys containing hard inclusions [1–7], few works focused on alloys with soft inclusions such as α/β two phases alloys [8,9]. The tensile flow properties of these alloys do not follow the classical linear law of mixture as uniform strain or as uniform stress [10,11]. In fact, the stress-strain behavior of two phases alloys depends on interaction stresses developed as a result of interactions between phases to maintain plastic strain compatibility. It has been recognized that the Bauschinger effect which results from these interactions is much more pronounced in the two phases alloys than in single phase polycristals [10]. The relation between the back stress X (measurement of the Bauschinger effect) and metallurgical parameters (morphology, size, distribution and volume fraction of phases and crystallographic relationships between phases) has been extensively studied [8,10]. However, the influence of the back stress on the void nucleation process is still misunderstood. The aim of this paper is to clarify the influence of metallurgical and mechanical parameters on the cavity nucleation process in α/β two phases titanium alloys.

2. MATERIALS AND SIMPLE DESCRIPTION OF THE DIFFERENT LEVELS OF HETEROGENEITY

Three α/β titanium alloys were studied : the TD5AC, Ti-6246 and TA6V alloys. The latter presents two different microstructures which result from various heat treatments (TA6Vg and TA6Va). The detailed chemical compositions and heat treatments for each alloy are given elsewhere [9,12]. In particular, all the materials studied have the same content of aluminum (5% wt). The microstructure of these alloys is composed of a primary α-phase (h.c.p. soft phase) surrounded by a β-phase (b.c.c. hard phase). The β-phase can be transformed (in Ti-6246, TA6Vg) and is then composed of a mixture of residual β-phase and secondary α-phase (α_s). Some morphological and mechanical parameters are reported in table 1.

Table 1: Morphological and mechanical parameters of the four α/β titanium alloys. The following hardening law has been chosen: $\Sigma = \Sigma_0 + K(\varepsilon p)^n$ where Σ_0 is the yield stress.

Nuances	E (GPa)	Σo(2E-4)	Σmax (MPa)	ε_l	ε_d	n	K (MPa)	%α	%β	$\phi\alpha$ (μm)	$\phi\beta$ (μm)
TA6Vg (300K)	130.2	912.2	1072.6	0.165	-0.25	0.43	453.4	47	52	15.0	-
TA6Va (300K)	110.0	900.0	1120.2	0.134	-0.23	0.3	479.5	50	50	5.0	200
6246g (773K)	109.6	740.8	1004.0	0.10	-0.38	0.75	7646	33	67	5.7	500
TD5AC (300K)	121.4	795.0	987.0	0.21	-0.40	0.421	475.5	28	72	1.5	500

The h.c.p. texture is similar for all the alloys studied and was previously described [9,12]. An important number of heterogeneity levels are generally observed in α/β titanium alloys (prior-β grains, two phases (α_p and β), transformed β structure, α_2 (Ti_3Al) precipitation in the α-phase, ...) [8,9,13]. Plastic strain incompatibilities which result from these microstructural heterogeneities, induce important internal stresses. This explains the high value of the back stress generally observed in α/β two phases alloys [10,13].
Recently, the importance of elasto-plastic behaviors of the two phases and the α-phase crystallographic texture on tensile and cyclic properties has been demonstrated [13,14]. It was shown, in particular, that the microstructure of an α/β two phases alloy can be considered as a aggregate of cells (figure 1). Where the cell is defined as an α crystal surrounded by a β-phase; the orientation of the cell is defined by the orientation of the associated α-platelet. The notion of cell is introduced to separate the internal stresses (X_{cell}) linked to the α-phase texture with the internal stresses ($X_{\alpha/\beta}$) linked to the difference between the elasto-plastic behaviors of the two phases, α and β. To sum up, we can state that the macroscopic back stress (X) is associated to three levels of plastic strain incompatibilities :

X_c : incompatibility between cells containing α particles with different crystallographic orientations ;

$X_{\alpha\beta}$: incompatibility between the soft phase α and the hard one β.

X_α : incompatibility associated to a heterogeneous plasticity in the α particle (walls, shear bands, ...);

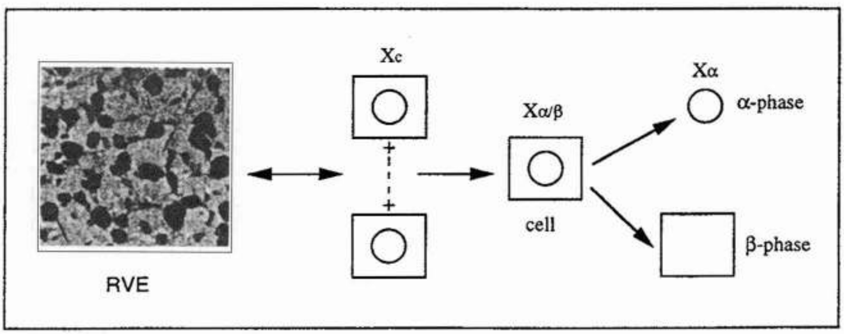

Figure 1: Schematic representation of an α/β titanium alloy with its heterogeneity levels (micrograph of the 6246 alloy). RVE is the representative volume element.

3. TENSILE BEHAVIOR : BACK (X) AND EFFECTIVE (Σ_{ef}) STRESSES

The tensile behaviors of the four alloys studied is described in Table 1. In the literature, it is usual to separate the macroscopic stress Σ in two components : the back stress (X) and the effective stress (Σ_{ef}). The back stress is generally associated with a local straining process which induces a long range interaction between mobile dislocations and the effective stress is the stress required locally for a dislocation to move. This stress partition, previously proposed by Cottrell [15] and Prager [16], and extensively discussed in the past by different authors [17–19] is done, in tensile loading, on each stress reversal at different plastic strains (figure 2). The change in back and effective stresses *vs* plastic strain is plotted in figure 3a.

The saturated value of the effective stress is obtained more rapidly than back stress saturation. Effective and back stresses saturation values are reported in figure 3b for each alloy. The effective stress saturated value seems to be constant for the different alloys studied. The differences observed on tensile behavior are mainly associated to the back stress components described above. For the alloys studied here, the plastic deformation is homogeneous in the α-phase until plastic strain remains weaker than 6% [12], then X_α is negligible. Besides, the α-phase texture is similar for the different alloys then X_c is constant. It can be concluded that the difference of back stress measured, depending on the alloy, results only from incompatibilities developed between the two phases, *i.e.* $X_{\alpha/\beta}$. The connection between back stress and the different levels of heterogeneities has been extensively studied previously [15,17–19]. However, the influence of back stress on nucleation process is a point which stays unclear.

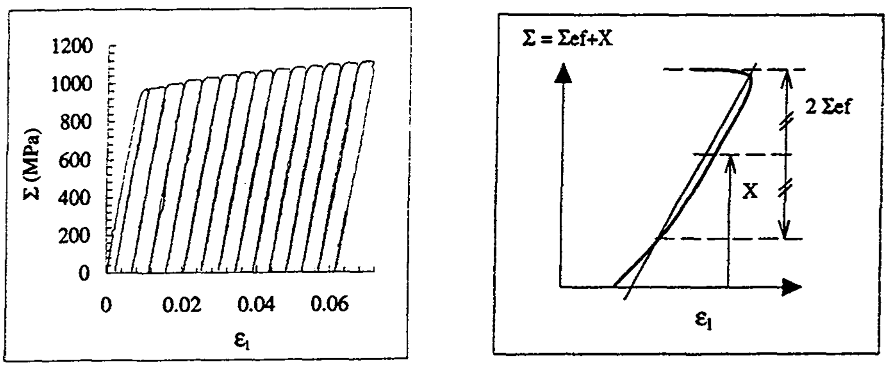

a) b)

Figure 2: a) Stress reversals at different strains. b) Stress partition as proposed by Cottrell.

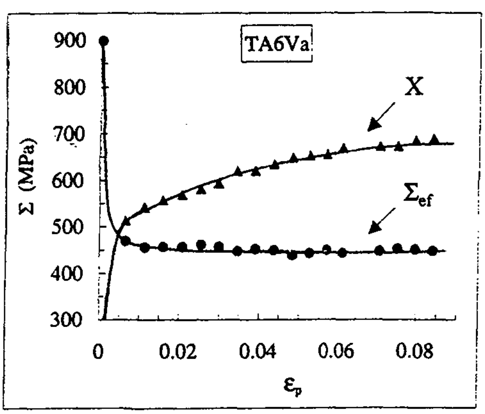

Alloys	Σs (MPa)	Σef (MPa)	Xs (MPa)
TA6Vg (300K)	1110	467.0	643.0
TA6Va (300K)	1124	450.0	674.0
6246g (773K)	1004	391.2	612.8
TD5AC (300K)	956	409.0	547.0

a) b)

Figure 3: a) Change in back and effective stresses with plastic strain during loading (TA6Va). b) Saturated values of the macroscopic stress Σ, the effective stress Σef and the back stress X.

4. NUCLEATION PROCESS IN THE α/β TITANIUM ALLOYS

4.1 The local approach of fracture

4.1.1 Calculation

The local approach of fracture has been used for the void nucleation study of the four α/β titanium alloys. This method was largely described on steels and aluminum [4-6,20] and allows to examine a wide range of triaxialities with the use of axisymetric notched specimens labeled AE2, AE4 and AE10. As far as the damage is studied under high and low triaxiality, smooth specimens (TL) were also used. These specimens were tested to fracture or interrupted before fracture. Besides, a finite element calculation was performed for each specimen design to provide the mechanical parameters distribution in the bulk of the specimen during loading up to fracture. During loading, the mesh is reorganized so as to take into account displacement. For each material, an elasto-plastic law is identified, from the plastic behavior of the alloy before necking, in the framework of the classical elasto-plastic theory, based on the thermodynamics of irreversible processes with internal variables (R and $\underline{\underline{X}}$) [21]. It has been experimentally demonstrated that it was not necessary to take into account damage in the behavior law since, just before fracture, the hydrostatic part of strain ε_{kk} remains lower than 0.0025. The plastic flow is expressed as function of the stress $\underline{\underline{\Sigma}}$, the kinematic hardening $\underline{\underline{X}}$, and the initial yield stress Σ_0:

$$\dot{\underline{\underline{\varepsilon}}}_p = \left\langle \frac{f}{K} \right\rangle^n \frac{\partial f}{\partial \underline{\underline{\Sigma}}} = \dot{p}\frac{\partial f}{\partial \underline{\underline{\Sigma}}} \quad \text{with} \quad f = J_2(\underline{\underline{\Sigma}} - \underline{\underline{X}}) - R - \Sigma_0 \;\; (f \le 0)$$

$$J_2(\underline{\underline{\Sigma}} - \underline{\underline{X}}) = \sqrt{\frac{3}{2}\left(\underline{\underline{S}} - \underline{\underline{X}}\right) : \left(\underline{\underline{S}} - \underline{\underline{X}}\right)} \quad \text{with } \underline{\underline{S}} \text{ the deviatoric part of } \underline{\underline{\Sigma}}$$

$$R = Q\,(1 - \exp(-bp))$$

$$\underline{\underline{X}} = \underline{\underline{X}}_1 + \underline{\underline{X}}_2 \quad \text{with} \quad \forall i \in \{1,2\},\; \dot{\underline{\underline{X}}}_i = \frac{2}{3} C_i \dot{\underline{\underline{\varepsilon}}}_p - \gamma_i \underline{\underline{X}}_i \dot{p}$$

Then, the variables of this law are: Σ_0, K, n, Q, b, Ci, γi, $\forall i \in \{1,2\}$. K and n are constants related to the viscosity. They have been chosen so as to simulate a time-independant behavior.
The validity of such calculations was checked comparing the experimental and calculated loading curves (figure 4) of notched specimens. The identification of the plastic law as described above allows the determination, after necking, of accurate calculated loading curves for smooth specimens (TL) (figure 5). Figure 5 shows the good agreement between calculated and experimental displacements during loading up to fracture. This macroscopic validity can be completed by a microscopic analysis of the local plastic strain of the α-particles measured from their change in shape [9,22]. As far as this local plastic strain is close to the calculated one, calculations are satisfactory.

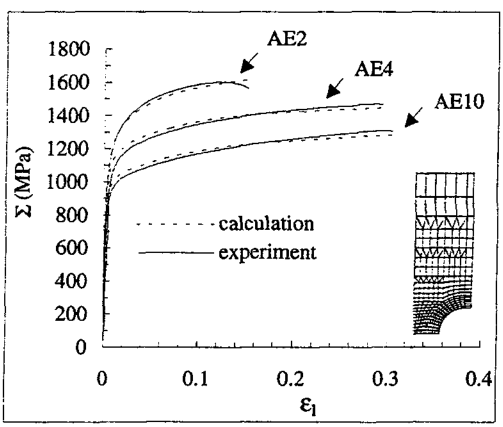

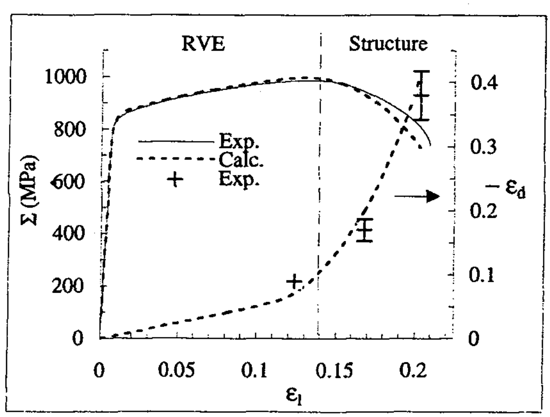

Figure 4: Experimental and calculated loading curves (Σ *vs* ε_l) for notched specimens (TD5AC).

Figure 5: Experimental and calculated loading curve (Σ *vs* ε_l) for the smooth specimen. Good agreement between experimental and calculated deformations after necking (TD5AC). ε_l is the longitudinal deformation and ε_d is the diametral deformation.

4.1.2- Damage observations

In order to understand void nucleation, a quantitative damage analysis was done in the midsection of the specimens. The specimens were longitudinally cut, mechanically polished and etched. For a better understanding of void appearance during loading, void maps were drawn in the necked sections of interrupted specimens [4,9]. Limits between regions containing cavities were identified assuming that under 8 voids/mm^2 the area is not considered as damaged. These void nucleation limits are characterized by the mechanical parameters such as ε_{peq} (the von Mises equivalent plastic strain), Σ_{equ} (the von Mises equivalent stress), Σ_m (the hydrostatic stress) or χ (the stress triaxiality state).

4.2 Nucleation events

Several nucleation events were previously described and quantified for α/β two phases alloys [8,9]. Voids can either form in the α-phase, in the β-phase, in twins or at the α/β interface. It was clearly shown that twins as well as voids in β remain negligible [9]. Most voids nucleate within the α-grains or at the α/β interface. As α-grain voids are present in few alloys (which α-grains contain dislocation subboundaries before loading), the nucleation criterion of α/β voids will be compared for the different alloys.

4.3 Nucleation criterion

Nucleation limits of voids located at the α/β interfaces were identified for the different alloys studied. Figure 6 shows the change of hydrostatic stress as a function of plastic strain along these nucleation limits. It is worth emphasizing that the nucleation strain (ε_{peq}) for these kind of voids strongly depends on triaxiality and plastic strain. The nucleation plastic strain increases when the hydrostatic stress (Σ_m) decreases. For each material, a critical hydrostatic pressure P_c can be defined under which no void nucleate whatever the plastic strain. For hydrostatic pressures lower than P_c, fracture occurs by nucleation and multiplication of micro-shear bands [9]. Besides, for a given hydrostatic pressure over P_c, the plastic strain needed for nucleation depends on the alloy.
The influence of hydrostatic pressure on void formation has been largely studied in alloys which contain hard inclusions [2,4,23-25]. These inclusions constitute favorite void nucleation sites. Fisher and Gurland [23,24] proposed a model which combines energy and stress criteria to give two conditions for void formation in spheroidized steels. In fact, it is generally assumed that cavity formation takes place for a local critical stress σ_c in the inclusion or at the inclusion-matrix interface when particles are large (> 1µm) [2,4] and it follows an energetic criterion when particles are small (< 20 nm) [23-25].

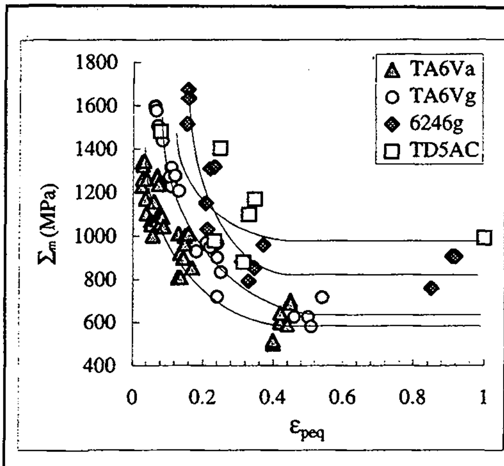

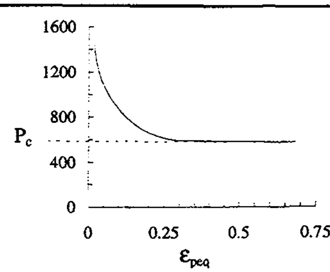

Alloys	Pc (MPa)
TD5AC	990
6246	819
TA6Vg	638
TA6Va	600

Figure 6: Hydrostatic stress needed for void nucleation at the α/β interface *versus* plastic strain. Critical hydrostatic stress, Pc, for the different alloys, under which no void nucleate.

Even if the notion of a critical stress at the interface seems to be accurate for α/β titanium alloys, since voids are created at the α/β interface, all these models assumed that the inclusion remains elastic which is not the case of the α-phase [13,26-28]. Moreover these criteria do not take into account the different heterogeneity levels present in α/β titanium alloys.In a first time, it appears necessary to discuss the macroscopic cavity nucleation criterion (figure 6) with a microscopic point of view. Then, it remains to determine what mechanical parameters, depending on the heterogeneity levels, may influence the nucleation process.

5. INFLUENCE OF MICROSCOPIC PARAMETERS ON VOID FORMATION

5.1 Cavity location and influence of σ_m

Studies on nodular cast iron alloys [29-31] show that void initiation occurs at the bottom and the top of the inclusion whereas for α/β titanium alloys, voids are mainly observed on both sides of the α-grains (figure 7). The main difference between these two cases is the behavior of inclusion and matrix which are reversed. In the case of the cast iron, the inclusion remains elastic and the matrix has an elasto-plastic behavior. In the case of titanium alloys, the α-grain (which is compared to the inclusion) is considered as the soft phase whereas the β-phase (matrix) is the hard phase. Two finite element calculations, on a mesh constituted of a spherical particle surrounded by a matrix (figure 7), were realized using whether the cast iron laws [29,30] or the titanium laws [11]. For both calculations, at a given macroscopic plastic strain, the only parameter which consequently varies along the interface from the particle's side to the particle's top is σ_m (the local hydrostatic stress). Indeed, for the same plastic strain of 0.03, the hydrostatic stress σ_m is maximum at the bottom and top of the inclusion in the case of the hard inclusion, whereas it is located at the inclusion's sides for the soft inclusion (figure 7). These regions of maximum pressure correspond to the places where voids are formed depending on the alloy studied. The influence of the local hydrostatic stress on the nucleation process at the α/β interface is then obvious.

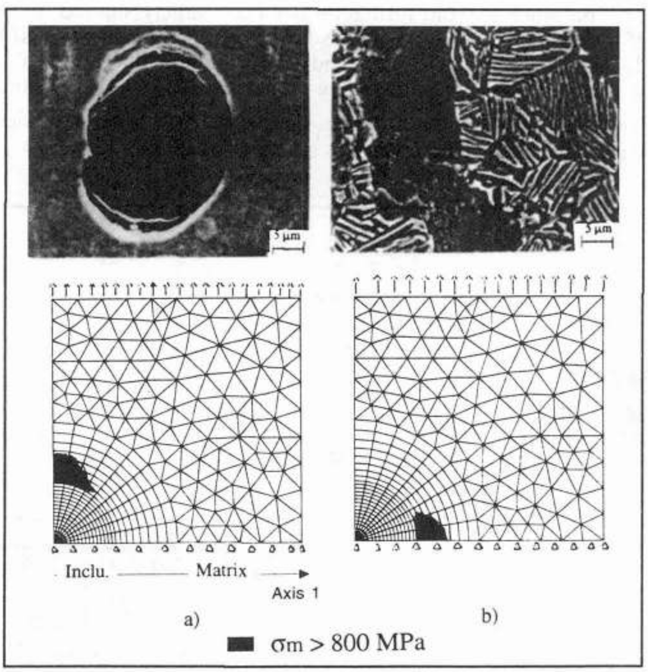

Figure 7: Void micrograph and calculated hydrostatic pressure for a) a cast iron and b) an α/β titanium alloy (TA6Vg). The maximum of σ_m corresponds to the place where void nucleate.

For the alloys studied, which contain numerous heterogeneities, the local hydrostatic stress developed in the vicinity of the α/β interface, depends on the macroscopic hydrostatic stress Σ_m but also on the multiaxial stress state present as a result of the plastic strain inhomogeneity between the two phases [32,33]: $\sigma_m = f(\Sigma_m$, heterogeneities). Thus, the fact that the fracture of the α/β interface depends on the local hydrostatic stress σ_m explains the dependence of the nucleation criterion on the macroscopic stress Σ_m.

5.2 The part of plastic strain in void nucleation

The fact that void nucleation at the α/β interface depends on Σ_m has been demonstrated. Nevertheless, Σ_m is not the only parameter involved in nucleation as shown in figure 6. The nucleation process also needs plastic strain. Using the Electron Backscattering Pattern (EBSP), the local influence of plasticity has been checked for the Ti-6246 alloy [12,34]. This method allows to associate a cavity with the crystallographic orientation of the α-particle in which the cavity has developed. Figure 8 shows that the angle θ between the <c> axis of the damaged α-particles and the stress axis is greater than 45° whatever the triaxiality. It has been previously shown [13,33] that large plastic strain occurs in this particular range of crystallographic orientations (the α-particles are well oriented for the prismatic slip which is the easier slip). Thus, cavities will easily form in plastic strained α-particles which explain the macroscopic plastic strain dependence of the nucleation criterion. Moreover, it was shown, recently, with a micro-macro model that the α-particles develop all the more triaxiality that the angle between their <c> axis and the stress axis is close to 90° [33].

To conclude, the nucleation process acts in α-particles which present crystallographic orientation favorable to prismatic slip ($\theta > 45°$) *i.e.* high local plastic strain $\varepsilon^{\alpha}_{peq}$, and as a consequence a high local hydrostatic stress σ_m.

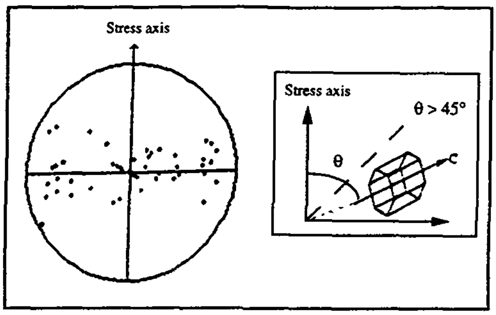

Figure 8: (0002) pole figure of the damaged α-particles in axisymetric specimens (6246).

6. INFLUENCE OF HETEROGENEITIES ON THE NUCLEATION CRITERION

6.1 The back stress: X

Critical pressures P_c, under which no void are created (figure 6) can be correlated to the saturated internal stress X_s of the different alloys (figure 9). For the alloys studied, P_c is defined for high plastic strains. For such plastic strains, X is saturated and equals X_s. It is then justified to associate P_c to X_s. The hydrostatic pressure needed for void nucleation at the α/β interface decreases when X_s increases. This result clearly shows the role of plastic strain incompatibilities developed in α/β titanium alloys on the nucleation process. This dependence on the internal stresses has been previously suggested by Beremin in A508 steels [4]. In this alloy, the nucleation process is associated to a local critical stress σ_c in the hard inclusions which is expressed as $\sigma_c=\Sigma_m+k(\Sigma_{equ}-\Sigma_o)$ where $k(\Sigma_{equ}-\Sigma_o)$ represents the internal stress arising from strain inhomogeneity between inclusion and matrix. This expression clearly shows that with high internal stresses (X), less hydrostatic stress will be necessary to reach the critical nucleation stress.
In α/β titanium alloys, the relationship between $\sigma_c^{\alpha/\beta}$, Σ_m and the internal stresses is not so clearly defined for the reasons expressed in part 4.3. Yet, some results are well established. Using the FEM [10] or a micro-macro model [33],it was shown that an increase in $X_{\alpha/\beta}$ involves an increase of local hydrostatic pressure σ_m in the α-phase. In particular, it has been explained that $X_{\alpha/\beta}$, and then σ_m, increase as a function of the following ratio: $C^*=\Sigma_0^{\beta}/\Sigma_0^{\alpha}$ [32].

A high value of internal stresses (X) will then increase the local hydrostatic stress σ_m. As a result, less macroscopic hydrostatic stress Σ_m will be necessary to reach the local criterion of void nucleation. This is precisely what is experimentally observed in figure 9.

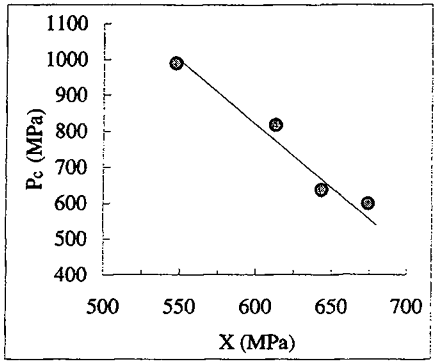

Figure 9: Change in hydrostatic stress needed for void nucleation with the back stress X.

6.2 The hardening rate dX/dεpeq

In the same manner, under high nucleation pressures (low plastic strains), it is interesting to study the influence of the hardening rate defined as $d\Sigma/d\varepsilon_{peq}$ on ε^a_{peq}. $d\Sigma/d\varepsilon_{peq}$ is close to $dX/d\varepsilon_{peq}$ since R is saturated for very small values of plastic strain. For a given Σ_m, it is possible to plot the change of ε^a_{peq} as a function of $dX/d\varepsilon_{peq}$ using the elasto-plastic laws of the four alloys. A nucleation criterion depending on $dX/d\varepsilon_{peq}$ and plastic strain is then defined for a fixed Σ_m (figure 10). This figure shows that the nucleation plastic strain decreases as the hardening rate increases whatever the hydrostatic stress. This result has previously been evidenced under low triaxiality (TL) for two phases titanium alloys [35]. When $dX/d\varepsilon_{peq}$ is higher than 2300 MPa, void nucleation does not depend on hydrostatic pressure or hardening rate, and $\varepsilon^a_{peq} \approx 0.02$. This plastic strain is the needed strain to create cavity whatever the hydrostatic stress or the hardening rate.
For values of $dX/d\varepsilon_{peq}$ close to zero, ε^a_{peq} is high. This corresponds to the plateau observed in figure 6 ($\Sigma_m = f(\varepsilon_{peq})$). The nucleation criterion is then a function of Σ_m and $X_{\alpha/\beta}$ only. In the mid range of ε^a_{peq}, the criterion is a function of Σ_m and $dX/d\varepsilon_{peq}$. For a given Σ_m, the plastic strain needed for void nucleation is all the more high that the hardening rate decreases quickly (material 2 in figure 11). In fact, if the material hardending rate decreases quickly, the internal stresses in the α-phase also decrease rapidly. Hence, the local hydrostatic stress σ_m is low.

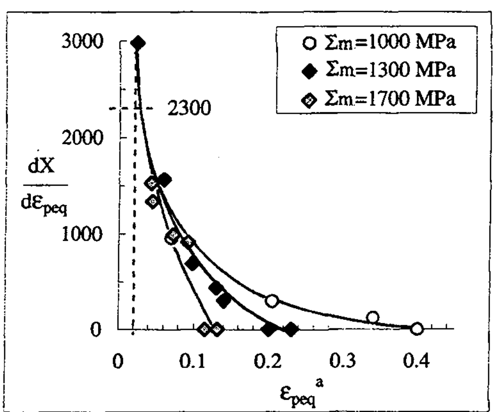

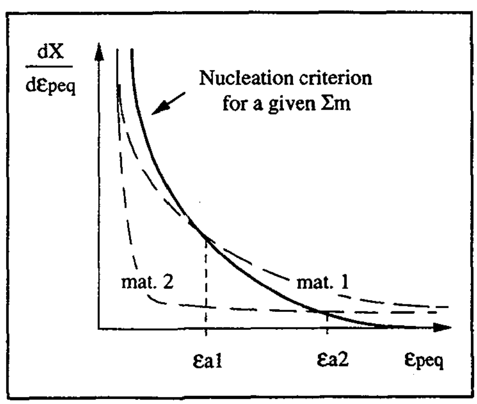

Figure 10: Plastic strain needed for nucleation as a function of the hardening rate for various hydrostatic stresses.
Figure 11: Comparison of the nucleation plastic strain between two materials reaching the same Xs more or less rapidly. Material 2 will nucleate later on.

If we assume the existence of a local nucleation criterion $\sigma_m=f(\varepsilon^{\alpha}_{peq})$, this material will need a high local plastic strain to create voids. Then, the nucleation plastic strain of this material (2) is quite greater than that of material 1.

6.3 Physical origin of X and dX/εpeq

From previous results [36,37] on α/β titanium alloys, it appears that the amount of secondary α-phase (α_s) is the main parameter driving the strengthening of the material. Then, following this result, FEM calculations were conducted to check the influence of the amount of α_s on the kinematic stress X and its rate $dX/d\varepsilon_{peq}$. The mesh used for calculation is the one described in part 5.1 (figure 7). Under various macroscopic plastic strains (maximum of ε_p=0.03), the stress gap between the inclusion (α) and the matrix (β) is a measurement of the kinematic stress $X_{\alpha/\beta}$ (figure 12 a). The kinematic rate will then be the slope of the curve $X_{\alpha/\beta}$ *versus* ε_{peq}. Our purpose is to check the influence of the α_s percentage on the kinematic stress and its rate. Also, the elasto-plastic law of the matrix β must be precisely defined as a function of the amount of α_s. In the following, it is assumed that the α_s-particles act as strong barriers for dislocations promoting an Orowan by passing process. A crude description of the behavior law of the β matrix may be written as follows:

$\Sigma_\beta = \Sigma_0^\beta + R_\beta + X_\beta$ in which

Σ_0^β is the yield stress of the β-phase.

R_β represents the increase of the yield stress linked to the α_s amount, then R_β is expressed as [38]:

$$R_\beta = \frac{\mu b}{\sqrt{\pi}}\sqrt{f}\left(\frac{A}{r}\right) = C\sqrt{f}$$

with b: the burgers vector of the b.c.c. β-phase, b=0.287 nm
μ: the shear modulus, μ = 45000 MPa
f: the surface fraction of α_s
r: the radius of the α_s-particles
A: a constant, A≈3

X_β takes into account the strain hardening process [39] under very small plastic strains: $X_\beta = X_0 + \mu f \varepsilon_p$. In fact, it was clearly demonstrated [40] that such an approach strongly overestimates the hardening since the spreading of strain tends to reduce the effective hardening rate. Then, instead of μ, a more appropriate value μ^* is generally taken as 10^{-2} to 10^{-1} μ.

Under such considerations, and taking into account results from the literature [11], the following behavior laws of the two-phases were obtained:

$$\Sigma_\alpha = 350 + 2800\,\varepsilon_p$$
$$\Sigma_\beta = 900 + C\sqrt{f} + (4800 + \mu^* f)\,\varepsilon_p$$

The value of C can be calculated taking r = 0.1 μm for the α_s-particle radius as measured with image analysis [41], then C = 178 Mpa. This result is in agreement with recent results in titanium alloys (C = 183 MPa) [37]. Besides, experiments in titanium alloys have provided a μ^* value equal to 6000 MPa [37]. This value lies in the range previously defined *i.e.* 10^{-1} μ. Such an approach is then considered as physically supported. Figure 12 b) shows the results obtained as a function of the α_s amount. The kinematic parameter and its rate increase with the α_s percentage. It is worth noting that the values of $dX/d\varepsilon_{peq}$ (sketch figure 12 b) agree with those experimentally obtained for nucleation (figure 10).
As a conclusion, an increase of secondary α-phase induces an increase of the hardening rate and then a decrease of the nucleation strain ε^{a}_{peq}. Such an increase is also at the origin of the increase of X and so a decrease of P_c.

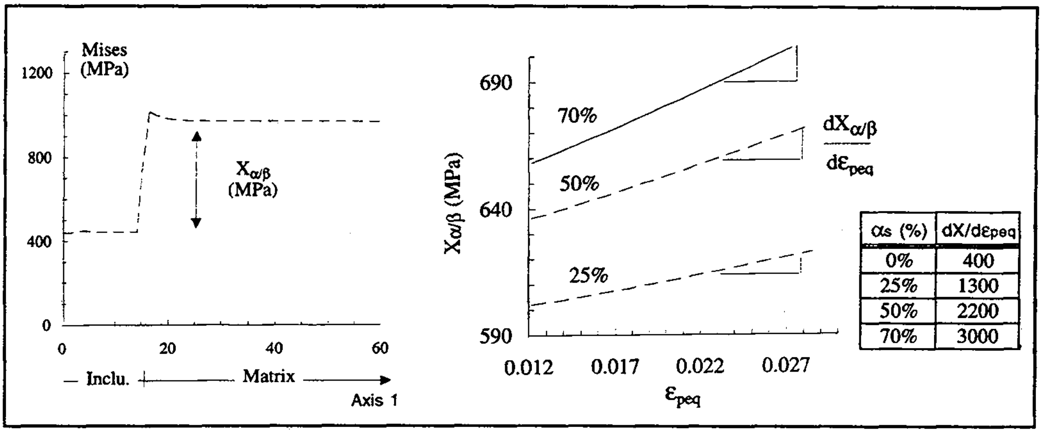

a) b)

Figure 12: a) Change in von Mises equivalent stress along the axis 1 (from inclusion to matrix). Determination of $X_{\alpha/\beta}$ as the stress gap. b) Increase of the kinematic rate as a function of the α_s amount.

7. CONCLUSION

The macroscopic void nucleation criterion for α/β titanium alloys is written as $\Sigma_m=f(\varepsilon_{peq})$. Besides, the strong influence of plastic strain in the α-phase and local hydrostatic stress on void formation has been evidenced. These two considerations support the existence of a local criterion $\sigma_m=f(\varepsilon^{\alpha}_{peq})$ of void initiation. Nevertheless, a direct link between the macroscopic and microscopic criteria is not obvious since the materials studied here contain numerous heterogeneity levels. In the future, we expect from a recent micromechanical model, to connect the macroscopic nucleation criterion of α/β voids with a microscopic one.

The role of plastic strain incompatibilities, developed as a result of heterogeneity levels, on the nucleation criterion, has been proved using the parameters : X and $dX/d\varepsilon_{peq}$. The following points must be summed up:

- The hydrostatic stress, P_c, under which no voids are created, decreases as the internal stresses (X_s) increase.
- The plastic strain needed for nucleation, ε^{a}_{peq}, increases as the hardening rate decreases, at a given Σ_m.
- For high values of Σ_m, ε^{a}_{peq} remains constant whatever $dX/d\varepsilon_{peq}$ and equals 0.02.
- For high values of $dX/d\varepsilon_{peq}$, ε^{a}_{peq} remains constant whatever Σ_m.
- For values of $dX/d\varepsilon_{peq}$ smaller than 2300 MPa, $\varepsilon^{a}_{peq}=f(\Sigma_m, dX/d\varepsilon_{peq})$.

References

[1]. J. Gurland, *Acta Met.*, **20** (1972) 735-740.
[2]. A.S. Argon, *J. Eng. Mater. Technol. Trans* ASME, **98** (1976) 60-68.
[3]. S.H. Goods and L.M. Brown, *Acta Met.*, **27** (1978) 1-15.
[4]. F.M. Beremin, *Met. Trans.*, **12A** (1981) 723-31.
[5]. A. Brownrigg, W.A. Spitzig, O. Richmond, D. Tierlinck and J.D. Embury, *Acta Met.*, **31**, No. 8, (1983) 1141-50.
[6]. J.W. Hancock and D.K. Brown, *J. Mech. Phys. Solids*, **31**, No. 1, (1983) 1-24.
[7]. R.H. Van Stone, T.B. Cox, J.R. Low, Jr, and J.A. Psioda, *Int. Met. Reviews*, **4** (1985) 157-179.
[8]. H. Margolin, J.C. Williams, J.C. Chesnutt and G. Lüetjering: *Titanium '80*, Science and technology, **1** (1980) 169-216.
[9]. A.L. Helbert, X. Feaugas, M. Clavel, *Met. Trans. A*, (1996) to be published.

[10]. L. Zhonghua, G. Haicheng, Met. Trans. A, part I and II, **21A** (1990) 717-732.
[11]. S. Ankem and H. Margolin: *Met. Trans.* A, **17** (1986) 2209-2226.
[12]. A.L. Helbert, X. Feaugas, M. Clavel, *Revue de Metallurgie*, (1996) to be Published.
[13]. X. Feaugas, P. Pilvin and M. Clavel, *Proceedings on the Zirconium 95 conference*, INSTN Saclay, France, April 1995.
[14]. P. Pilvin, X. Feaugas and M. Clavel, *Proceedings on the IUTAM conference*, Sèvres, France, October 1994.
[15]. A.H. Cottrell, *Dislocations and plastic flow in cristals*, Oxford University press, London, UK, (1953) *111-116*.
[16]. W. Prager, *J. Appl. Phys.*, **20** (1945) 235.
[17]. G.W. Kulhmann, D. Wilsdorf and C. Laird, *Mat. Sci. Eng.*, **37** (1979) 111-120.
[18]. S.I. Hong and C. Laird, *Mat. Sci. Eng.*, **128** (1990) 15-169.
[19]. J. Dickson, L. Handfield and G. L'Esperance, *Mat. Sci. Eng.*, **60** (1983) L3-L7.
[20]. J.A. Walsh, K.V. Jata and E.A. Starke jr: *Acta Met.*, Vol. **37**, No. 11 (1989) 2861-71.
[21]. J.L. Chaboche, *Int. J. Plasticity*, **5** (1989) 247-302.
[22]. M. Bourgeois, X. Feaugas and M. Clavel, *Scripta Met.*, **34** (1996).
[23]. J.R. Fisher and J. Gurland, Met. Sci., **15** (1981) 185.
[24]. J.R. Fisher and J. Gurland, Met. Sci., **15** (1981) 193.
[25]. K. Tanaka, T. Mori and T. Nakamura, *Philos. Mag.*, **21** (1970) 267.
[26]. Y. Saleh and H. Margolin, *Acta Metall.*, **27** (1978) 535.
[27]. C. H. Wells and C.P. Sullivan, *Trans.* ASM, **62** (1969) 263.
[28]. Y. Mahajan and H. Margolin: Part I and II, *Met. Trans.* A, **13** (1982) 267-274.
[29]. Y.Q. Sun and D. François, *Revue de Metallurgie* CIT, (1984) 809-817.
[30]. M. Dong, G.K. Hu, C. Prioul and D. Francois, MECAMAT93, *Int. Sem. on micromechanisms of materials*, France, Ed. Eyrolles, (1993) 511-521.
[31]. C. Guillemer-Neel, A.S. Beranger, M. Clavel, *Proceedings of the 11th European Conference on fracture* (1996), to be published.
[32]. L. Zhonghua, G. Haicheng, Met. Trans. A, **22A** (1991) 2695-2702.
[33]. X. Feaugas, Doctoral Thesis, U.T.C. France, (1994).
[34]. M. Bourgeois, X. Feaugas, M. Clavel, Private communication U.T.C. France, (1996).
[35]. T.V. Vijayaraghavan and H. Margolin, *Scripta Met.*, **23** (1989) 703-704.
[36]. G.T. Terlinde, T.W. Duerig and J.C. Williams, *Met. Trans. A*, **14A**, (1983) 2101.
[37]. D. Bourgarit, Private communication, (1996).
[38]. L.M. Brown, R.K. Ham, « Strengthening methods in cristals », Eds Halsted Press Division, John Wiley & Sons, New-York (1971).
[39]. D. Francois, A. Pineau and A. Zaoui, Comportement mécanique des matériaux, Tomes I et II, Ed. Hermès, Paris, (1993).
[40]. P. Pilvin, Doctoral Thesis, Paris-VI France, (1990).
[41]. D. Luquiau, X. Feaugas and M. Clavel, Private communication, (1996).